Check for updates

Bioelectromagnetics 43:106–118 (2022)

Effects of Acute Exposure to 3500 MHz (5G) Radiofrequency Electromagnetic Radiation on Anxiety-Like Behavior and the Auditory Cortex in Guinea Pigs

Honghong Yang,[1] Yuanyuan Zhang,[2] Xianwen Wu,[1] Ping Gan,[3] Xiaoli Luo,[1] Shixun Zhong,[1]* and Wenqi Zuo [1]*

[1]Department of Otorhinolaryngology, The First Affiliated Hospital of Chongqing Medical University, Chongqing, China
[2]Department of Otolaryngology-Head and Neck Surgery, Renmin Hospital of Wuhan University, Wuhan, Hubei, China
[3]Department of Dependable Service Computing in Cyber Physical Society, Key Laboratory of the Ministry of Education, Chongqing University, Chongqing, China

Numerous studies have shown that radiofrequency electromagnetic radiation (RF-EMR) may negatively affect human health. We detected the effect of 3500 MHz RF-EMR on anxiety-like behavior and the auditory cortex (ACx) in guinea pigs. Forty male guinea pigs were randomly divided into four groups and exposed to a continuous wave of 3500 MHz RF-EMF at an average specific absorption rate (SAR) of 0, 2, 4, or 10 W/kg for 72 h. After exposure, malondialdehyde (MDA) levels, antioxidant enzyme activity, anxiety-like behavior, hearing thresholds, cell ultrastructure, and apoptosis were detected. Our results revealed that hearing thresholds and basic indexes of animal behavior did not change significantly after exposure ($P > 0.05$). However, the MDA levels of ACx were increased ($P < 0.05$), and catalase (CAT), superoxide dismutase (SOD), and glutathione peroxidase (GSH-px) activities were decreased ($P < 0.05$) in the exposure groups compared to the sham group. Ultrastructural changes of ACx, including swollen mitochondria and layered myelin sheaths, were observed. Cytochrome-c relocalization, caspase-9, and cleaved caspase-3 activation were detected in the exposure groups. In conclusion, these results suggest that oxidative stress is an important mechanism underlying the biological effects of RF-EMR, which can induce ultrastructural damage to the ACx and cell apoptosis through a mitochondria-dependent mechanism. Moreover, oxidative stress, apoptosis induction and ultrastructural damage increase in a SAR-dependent manner. However, RF-EMR does not increase hearing thresholds or induce anxiety. Bioelectromagnetics. 43:106–118, 2022. © 2021 Bioelectromagnetics Society.

Keywords: apoptosis; anxiety-like behavior; auditory cortex; oxidative stress; radiofrequency electromagnetic radiation

INTRODUCTION

Many devices such as microwave ovens, mobile phones, WiFi routers, and base stations produce radiofrequency electromagnetic radiation (RF-EMR) fields and thus affect our daily lives. RF-EMR seems to act as a toxin to biological systems. The hazardous effects of RF-EMR on the human body have long been a hot topic and are still controversial. It has been reported that RF-EMR produces adverse effects such as male fertility impairment [Wdowiak et al., 2007; Agarwal et al., 2009], increased brain cancer risk [Carpenter and Sage, 2007], and neuropsychological disorders including anxiety, tinnitus, fatigue, headache, drowsiness, and hypomnesis [Thomée et al., 2011; Dasdag et al., 2015; Calvente et al., 2016; Wang et al., 2017]. However, there is no consensus

Grant sponsors: The Foundation and Frontier Research Project, Science and Technology Commission, Yuzhong District, Chongqing, China, grant number: 20180105; the Science and Technology Research Program of Chongqing Municipal Education Commission, grant number: KJQN201900433; the National Nature Science Foundation of China, grant number: 81700916.

Conflicts of interest: None.

*Correspondence to: Shixun Zhong and Wenqi Zuo, Department of Otorhinolaryngology, The First Affiliated Hospital of Chongqing Medical University, 1 Youyi Road, Yuzhong District, Chongqing 400016, China. E-mail: zhongsx@sohu.com; zuowenqi@163.com

Received for review 4 December 2020; Revised 26 September 2021; Accepted 5 January 2022

DOI:10.1002/bem.22388
Published online 23 January 2022 in Wiley Online Library (wileyonlinelibrary.com).

© 2021 Bioelectromagnetics Society

regarding whether RF-EMF exposure could cause potential detrimental effects in living animals or isolated brain regions.

Frequency and specific absorption rate (SAR) are two important indexes used to measure RF-EMR. Previous studies have revealed that exposure of developing rodents to RF-EMR may lead to an impairment of brain cells, which depends on variables such as the target-SAR and the duration and frequency of EMF exposure. The frequency of RF-EMR produced by communication devices such as mobile phones and base stations is typically 800–2000 MHz [Valberg et al., 2006]. However, 5 G (450–3800 MHz and 24–80 GHz) mobile phones are increasingly being used. The SAR is defined as the amount of RF-EMR energy absorbed by body tissues (watts per kilogram, W/kg). The biological impact of RF-EMR can be classified as thermal and nonthermal. Thermal effects are related to the heat created by RF-EMR, while nonthermal effects are associated with energy absorbed by tissues [Leszczynski et al., 2002; Challis, 2005]. According to the criteria of the Institute of Electrical and Electronics Engineers standard, the SAR limit value of mobile phones is 2 W/kg in most European countries, but in the United States, it is 1.6 W/kg [Hardell and Sage, 2008]. According to the guidelines of the International Commission on Non-Ionizing Radiation Protection (ICNIRP), the whole-body average SAR and the localized (head and trunk) SARs of occupational and general public exposure are 10, 0.08, and 2 W/kg, respectively. Additionally, RF-EMR at an SAR of 4 W/kg has a thermal effect [Vecchia, 2007; Hardell and Sage, 2008].

The ear and auditory cortex (ACx) of the brain are the most exposed areas to RF-EMR when holding a wireless cell phone to ear [Angela et al., 2003; Dimitris et al., 2013; Chen et al., 2014]. The effect of RF-EMR on hearing and the ACx is controversial. Seckin et al. [2014] reported that exposure to 900 MHz RF-EMR induces significant ultrastructural destruction of the cochlear. Oktay et al. [2004] and Oktay and Dasdag [2006] demonstrated that occupational or long-term exposure to electromagnetic radiation fields can lead to sensorineural hearing loss. However, some studies have shown contrary results [Ozturan et al., 2002; Uloziene et al., 2005; Sievert et al., 2007]. Additionally, our previous study demonstrated ultrastructural changes in spiral ganglion neurons (SGNs) and increased expression of autophagy biomarkers following exposure to RF-EMR at 1800 MHz and 4 W/kg after lipopolysaccharide (LPS) treatment [Zuo et al., 2015].

Redox homeostasis plays an important role in maintaining the normal physiological functions of the body. A change in the cellular redox balance and overproduction of reactive oxygen species (ROS) are part of signal transduction pathway during apoptosis. In addition, mitochondria are critical for normal cognitive function in animals; therefore, apoptosis may be one of the main factors involved in RF-EMR-induced cognitive changes [Tanaka et al., 2008; Gupta et al., 2018].

Based on these studies, we hypothesize that oxidative stress is an important mechanism underlying the bioeffects of RF-EMR, which may further activate the apoptotic pathway and affect hearing and anxiety-like behavior. The ACx is increasingly understood to be an integral part of the network of brain regions responsible for prediction, auditory perceptual decision-making, and learning, which play vital roles in the perceptual processing of complex acoustic stimulus [King et al., 2018]. The bioeffects of RF-EMR on the function of different organs, such as the hypothalamus [Dundar et al., 2009], hippocampus [Gupta et al., 2018], the ear canal [Akdag et al., 2018], cochlea [Yorgancilar et al., 2012; Zuo et al., 2015], and cochlear nuclei [Özgür et al., 2015], have been widely investigated. However, few studies have investigated the effects of RF-EMR on the ACx. In recent years, the hazards of long-term exposure to RF-EMR have been a research hotspot, but acute damage to the ear and ACx caused by RF-EMR has not been well studied. We detected cellular ultrastructure and apoptosis in the ACx by transmission electron microscopy (TEM) and immunofluorescence (IF), respectively, evaluated anxiety-like behavior by using the open field test (OFT), and assessed hearing thresholds by measuring auditory brainstem response (ABR) thresholds following RF-EMR exposure at three different SARs (2, 4, and 10 W/kg). In addition, malondialdehyde (MDA) levels and catalase (CAT), superoxide dismutase (SOD), and glutathione peroxidase (GSH-px) activities in the ACx were analyzed to assess the effects of RF-EMR on lipid peroxidation and oxidative stress.

MATERIALS AND METHODS

Animals

Forty adult male guinea pigs (body mass: 300–350 g) with normal hearing were obtained from the animal center of Chongqing Medical University (China) and kept in a humidity-controlled environment (55% ± 10%) at room temperature (20–22 °C) under a 12/12 h light/dark cycle. The animals were

1521186x, 2022, 2, Downloaded from https://onlinelibrary.wiley.com/doi/10.1002/bem.22388 by University Of British Columbia, Wiley Online Library on [10/10/2026]. See the Terms and Conditions (https://onlinelibrary.wiley.com/terms-and-conditions) on Wiley Online Library for rules of use; OA articles are governed by the applicable Creative Commons License

acclimatized for 1 week before the experiments. All experiments were approved by the Ethics Committee of Chongqing Medical University of China and were performed in accordance with the National Research Council Guide for the Care and Use of Laboratory Animals.

Exposure System

The 3500 MHz electromagnetic radiation exposure system was designed and built by the Department of Dependable Service Computing in Cyber Physical Society (Key Laboratory of the Ministry of Education, Chongqing University, Chongqing, China) (Fig. 1). To ensure the stability and reliability of the exposure, the exposure system was calibrated by N9010A EXA Signal Analyzer (Agilent Technologies, Palo Alto, CA) before exposure. The animals were kept in a wooden cage having dimension of $40 \times 40 \times 60$ cm with sufficient free space during the exposure of EMR. The carbon sheets impregnated with Styrofoam covered the upper surface and base of the cage in order to minimize the reflections of electromagnetic radiation. After that, the wooden cage was placed and fixed in an anechoic chamber with a size of $60 \times 60 \times 80$ cm, which was filled with Styrofoam radiation absorber (to reduce the reflection of radiation to the horn antenna).

The radiation exposure system consisted of a microwave signal source (USRP-2900; National Instruments, Austin, TX), amplifier (Hengzhi, Chengdu, China), horn antenna (A-INFO, Chengdu, China), wave guide transition (Hengzhi), computer system, power sensor, and power meter (No. 836 A; Agilent Technologies), as described in detail in a previous paper [Wang et al., 2017]. The horn antenna (A-INFO) was kept in such a manner that it received uninterrupted radiation from the source. The temperature of anechoic chamber was kept constant 25 ± 2 ℃ throughout the exposure period. The setup also has a power meter with power sensor to measure the maximum output power. This was measured to be 19.9 dBm which was delivered to the horn antenna and amplifier. The distance between the pyramidal horn and the mid plane of animal's body was estimated by far field formulae ($R \geq 2D^2/\lambda$) to be 60 cm. The power input to the horn antenna and the reflections were measured by using a 20 dB cross-coupler, power sensor, and power meter of range 30 lm to 3 W. The power that was transmitted (Pt) to the antenna was estimated by subtracting the reflected power with input power, which was sent to the software-controlled computer system.

The power density was obtained by using the following formula: Power Density = PtGt/4pR2, where Pt is the power transmitted into the cage, Gt is the gain of the horn, and R is the distance

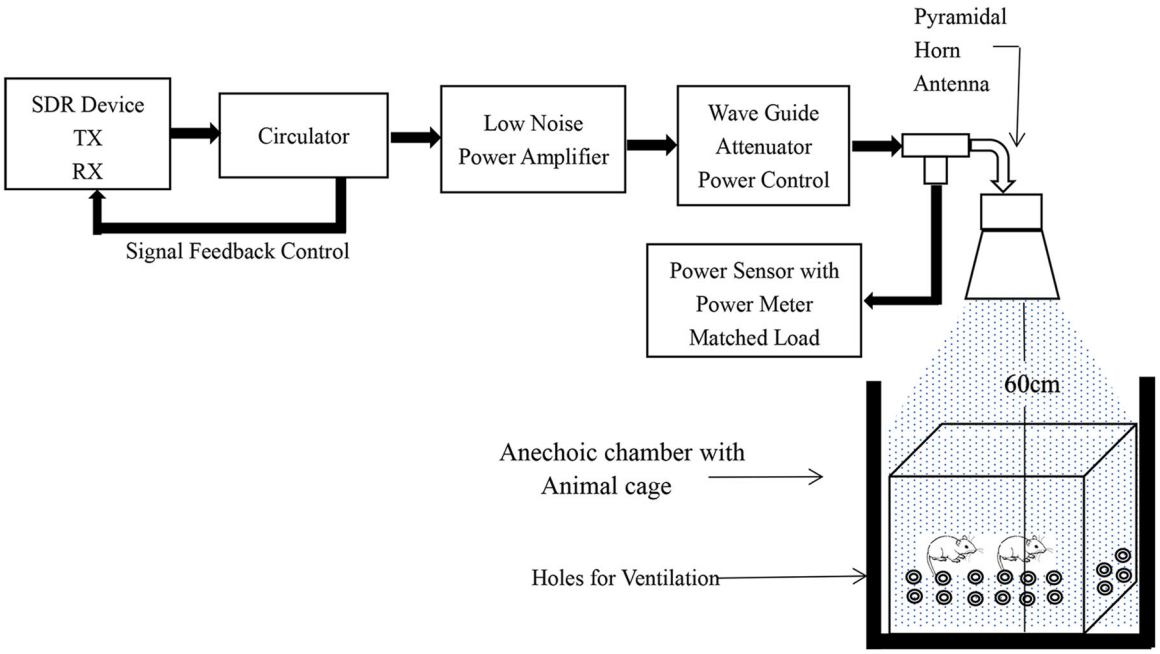


Fig. 1. RF-EMR-exposure system (detailed description in text). RX = Receive Port; SDR Device = NI radiation resource; TX = Transmit Port. Circulator. Power Amplifier. Wave guide attenuator, Power sensor, Horn and antenna, anechoic chamber.

1521186x, 2022, 2, Downloaded from https://onlinelibrary.wiley.com/doi/10.1002/bem.22388 by University Of British Columbia, Wiley Online Library on [10/10/2026]. See the Terms and Conditions (https://onlinelibrary.wiley.com/terms-and-conditions) on Wiley Online Library for rules of use; OA articles are governed by the applicable Creative Commons License

between the horn aperture and mid plane of the rat in the cage.

Experimental Design

Forty guinea pigs were randomly divided into four groups ($n = 10$), i.e. the sham group, 2, 4, and 10 W/kg groups. Guinea pigs in the sham group were kept in a radiation box without being exposed to RF-EMR, and the others were exposed to 3500 MHz RF-EMR at different SARs for 72 h. During the exposure time, there were no limitations on food, drink, or activity.

Auditory Brainstem Response Thresholds

Four hours before and after exposure, ABR were conducted as previously described [Qin et al., 2017]. Hearing in both ears was evaluated in a soundproof room with Smart EP (Intelligent Hearing, Miami, FL) hardware and software before and after exposure based on ABR thresholds. Animals were anesthetized with pentobarbital (40 mg/kg), and then three electrodes were inserted subcutaneously, one (the active electrode) at the vertex and the other two (the ground and reference electrodes) at the muscles behind both auricles. The intensity was decreased from 80 dB SPL in 20-dB steps and then in 10-dB and 5-dB steps to obtain the threshold. The hearing threshold was defined as the lowest level that evoked a wave III response.

Open Field Test

One hour after the termination of exposure, open field tests were conducted. Anxiety-like behavior was evaluated as previously described [Fiset et al., 2015]. Due to thigmotaxis, rats and mice tend to walk along a wall. Animals that spend most of their time in the periphery are more anxious than those that explore the center [Tobach and Gold, 1966; Zipser et al., 2014; Fiset et al., 2015]. Each animal was placed in the center of a plexiglass box ($100 \times 100 \times 50$ cm) with a black floor for 15 min to measure parameters such as distance traveled, time spent in the inner zone, and average velocity. The data were recorded by a computer-controlled tracking system (Mobile Datum Information, Shanghai, China) under dim light. To eliminate odor cues, the box was cleaned with 70% ethanol before each test.

Measurement of MDA Levels and Antioxidant Enzyme Activity

The guinea pigs were sacrificed after completion of behavioral and ABR tests, and the ACx was removed quickly on ice and washed with ice-cold sterile 0.01 M phosphate-buffered saline (PBS). Then, the samples were diluted with PBS and centrifuged, and the supernatants were collected for estimation of oxidative stress parameters (MDA, GSH-Px, SOD, and CAT).

Estimation of Total Protein

Total protein concentrations were measured with a BCA Protein Assay Kit (Servicebio, Wuhan, China). Values were expressed in terms of per mg protein.

MDA

Lipid peroxidation was estimated spectrophotometrically by measuring the level of MDA. Briefly, 50 µl of 0.8% butylated hydroxytoluene (BHT), 750 µl 0.8% of TBA, 750 µl of 20% acetic acid (pH 3.5), and 100 µl of 8% SDS were added to 100 µl of tissue homogenate. The reaction mixture was then incubated at 95 °C, in water bath for 1 h. After this, the mixture was cooled down by keeping on ice for 15 min and then centrifuged at 2000 rpm for 10 min. Absorbance was taken at 532 nm. Values were expressed in terms of nmol/mg protein.

CAT Activity

Catalase was estimated by measuring the decomposition of hydrogen peroxide (H_2O_2). The reaction mixture contained 1.9 ml of 50 mM phosphate buffer (pH 7.0) and appropriate dilution of tissue supernatant to make a volume 2 ml. Reaction was initiated by addition of 1 ml of freshly prepared 30 mmol H_2O_2 and the decrease in absorbance was measured at 405 nm. One unit of catalase represents the decrease of 1 µM of H_2O_2 per min. Activity was expressed in terms of U/mg protein.

SOD Activity

In brief, the reaction mixture consisted of 100 µl of sample, 150 mM phosphate buffer (pH 7.4), 20 mM L-methionine, 50 µM EDTA, 1% Triton X–100, 100 µM riboflavin, and Greiss reagent. The absorbance was taken at 550 nm. Total SOD value was calculated in term of units defined as the amount of SOD that inhibits the reduction of nitroblue tetrazolium (NBT) by 50%. Activity was expressed in terms of U/mg protein.

Glutathione Peroxidase

The reaction mixture (1 ml) contained 50 µl sample, 398 µl of 50 mM phosphate buffer (pH 7.0), 2 µl of 1 mM EDTA, 10 µl of 1 mM sodium azide, 500 µl of 0.5 mM NADPH, 40 µl of 0.2 mM GSH, and 1U glutathione reductase. The resultant mixture was allowed to equilibrate for 1 min at room temperature. After this, the reaction was initiated by addition of

1521186x, 2022, 2, Downloaded from https://onlinelibrary.wiley.com/doi/10.1002/bem.22388 by University Of British Columbia, Wiley Online Library on [10/10/2026]. See the Terms and Conditions (https://onlinelibrary.wiley.com/terms-and-conditions) on Wiley Online Library for rules of use; OA articles are governed by the applicable Creative Commons License

100 mM H_2O_2. The absorbance measured kinetically at 412 nm for 3 min. Activity was expressed in terms of U/mg protein.

Transmission Electron Microscopy

Guinea pigs were anesthetized with pentobarbital and transcardially perfused with 0.01 M PBS (pH 7.4) and 2.5% glutaraldehyde. The ACx was removed quickly and fixed with the same glutaraldehyde solution overnight at 4°C and then postfixed with 1% osmium tetroxide for 2 h. The tissues were dehydrated in different concentrations of ethanol, treated with propylene oxide for 30 min, and then embedded in mixtures containing different concentrations of araldite. Ultrathin sections were placed on copper grids and stained with uranyl acetate followed by lead citrate. TEM (FEI TecnaiG212; Phillips, Eindhoven, Holland) was used to examine ultrastructure.

Immunofluorescence Staining

Animals were transcardially perfused with 0.01 M PBS and 4% paraformaldehyde after being anesthetized with intraperitoneal pentobarbital sodium. The brains were collected and fixed with 4% paraformaldehyde for 24 h at 4°C, embedded, sectioned at a thickness of 5 mm, and mounted on glass slides. The dewaxed sections were incubated with 10 mM citrate buffer (pH 6.0) for 5 min. Some sections were incubated with an anti-Cyt-*c* antibody (1:500; Servicebio, Wuhan, China), some sections were incubated with a cleaved caspase-3 antibody (1:500; Servicebio), and the others were incubated with a caspase-9 antibody (1:500; Servicebio) overnight at 4 °C. After three washes with PBS, all sections were incubated with the secondary antibody (1:500; Servicebio) at 37 °C for 1 h. Subsequently, the sections were examined under a laser-scanning confocal microscope (Nikon, Tokyo, Japan).

Statistical Analysis

The results were analyzed with SPSS 23.0 software (SPSS, Chicago, IL). ABR data were analyzed by paired *t* test, and other data were analyzed by one-way analysis of variance. All data are presented as the means ± standard deviation (SD), and $P < 0.05$ were considered statistically significant.

RESULTS

Auditory Function

As shown in Figure 2, there were no significant changes in ABR thresholds after exposure to different SARs (sham, 2, 4, and 10 W/kg), which indicates that acute exposure to RF-EMR does not increase the hearing threshold.

Exploratory Behavior

To evaluate exploratory behavior after exposure, the OFT was performed before the ABR test. As shown in Table 1, after exposure for 72 h, there were no significant differences in the distance traveled (m), the time spent in the inner zone (s), or the average velocity (cm/s) between the sham and exposure groups, which indicates that acute exposure to RF-EMR does not induce anxiety-like behavior in guinea pigs.

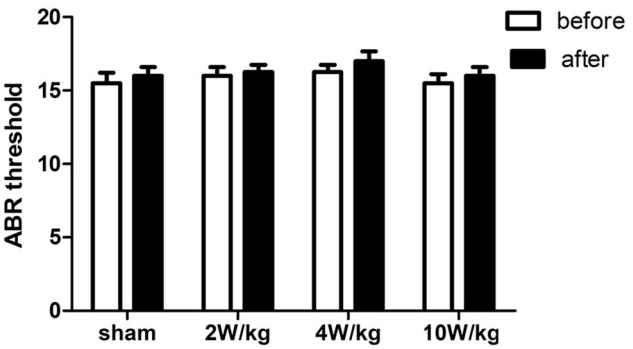


Fig. 2. The effect of 3500 MHz RF-EMR on ABR thresholds. There were no significant changes in ABR thresholds after exposure to RF-EMR at different SARs (sham, 2, 4, and 0 W/kg) ($P > 0.05$). ABR = auditory brainstem response; RF-EMR = radiofrequency electromagnetic radiation; SAR = specific absorption rate.

TABLE 1. The Effect of 3500 MHz RF-EMR on Open Field Test

	Sham	2 W/kg	4 W/kg	10 W/kg	*P*
Total distance (m)	136.34 ± 70.37	141.84 ± 62.57	130.08 ± 47.21	119.23 ± 36.78	0.82
Speed (cm/s)	15.15 ± 7.86	15.83 ± 6.98	14.45 ± 5.25	13.25 ± 4.09	0.82
Inner zone time (s)	50.11 ± 45.09	46.68 ± 38.42	20.33 ± 21.68	36.89 ± 34.02	0.26

Note: There were no significant differences in the distance traveled (m), the time spent in the inner zone (s), or the average velocity (cm/s) between the sham and exposure groups ($P > 0.05$). The values are expressed as the mean ± SD.

1521186x, 2022, 2, Downloaded from https://onlinelibrary.wiley.com/doi/10.1002/bem.22388 by University Of British Columbia, Wiley Online Library on [10/10/2026]. See the Terms and Conditions (https://onlinelibrary.wiley.com/terms-and-conditions) on Wiley Online Library for rules of use; OA articles are governed by the applicable Creative Commons License

Ultrastructural Morphology of the ACx

As shown in Figure 3, in the sham group, no obvious ultrastructural changes in ACx neurons were found. Intact nuclear membranes, normal mitochondria, and intact and compact myelin sheaths were observed (Fig. 3A, A1, A2). However, swollen mitochondria in neurons and layered myelin sheaths in nerve fibers were found in the exposure groups. In the 2 W/kg group, neuronal mitochondria were slightly swollen, while myelin sheaths were intact (Fig. 3B, B1, B2). In the 4 and 10 W/kg groups, mitochondria were swollen, and myelin sheaths were obviously layered. These changes were more significant in the 10 W/kg group (Fig. 3D, D1, D2).

Oxidative Stress Indexes in the ACx

To study the effect of RF-EMR on the ACx, the oxidative stress markers MDA, CAT, SOD, and GSH-px were detected. As shown in Figure 4, we found that the level of MDA was significantly increased, while the activities of CAT, SOD, and GSH-px were significantly decreased in the exposure groups compared to the sham group. In the 2, 4, and 10 W/kg groups compared to the sham group, the levels of MDA were increased by

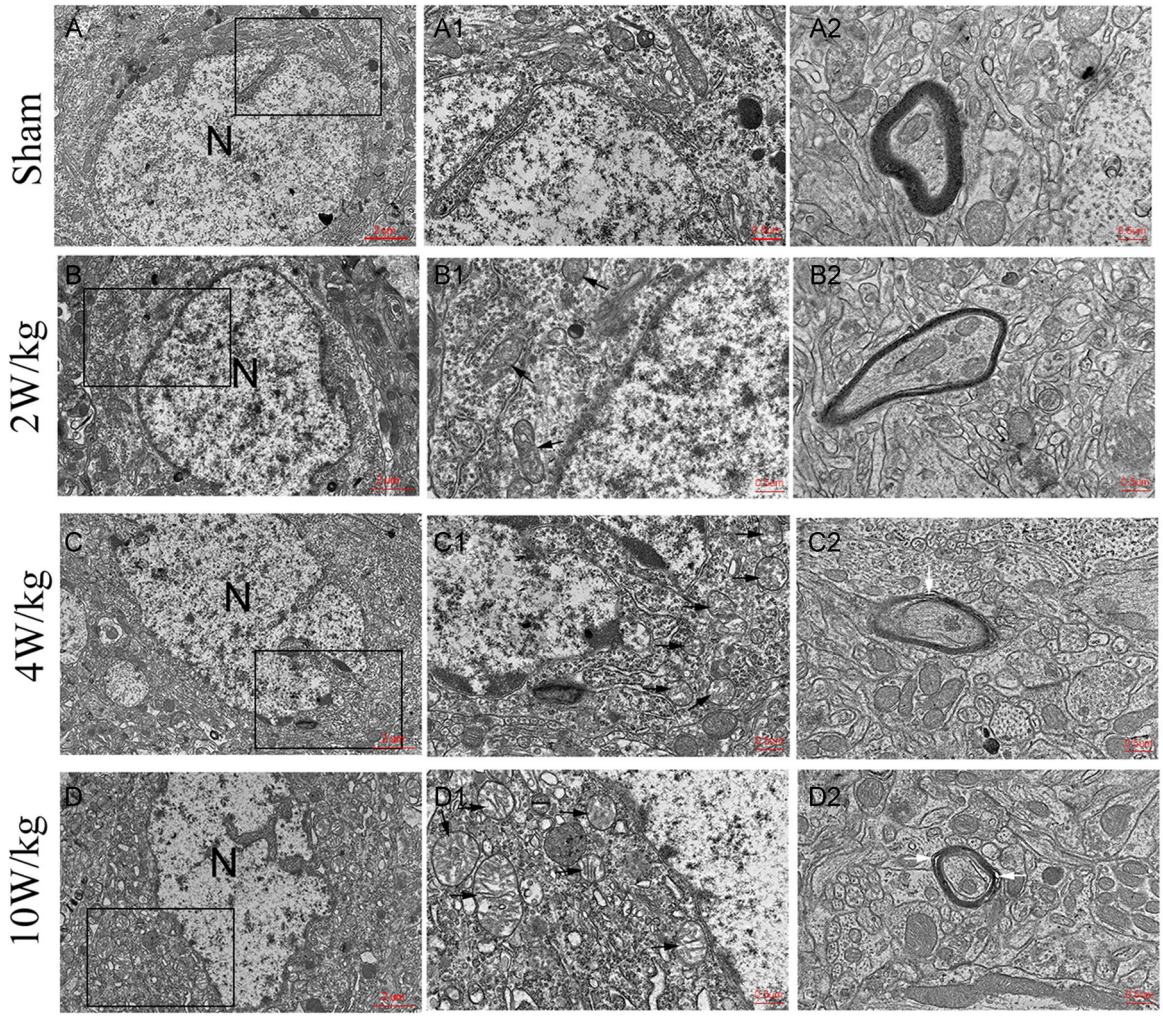


Fig. 3. The effect of 3500 MHz RF-EMR on the ultrastructure of the ACx (magnification, ×8000, ×20,000). Normal nucleus, uniformly chromatin, and normal mitochondria are shown in the sham group (**A1**), while swollen mitochondria (black arrows) were found in the 2, 4, and 10 W/kg groups (**B1**, **C1**, **D1**). Intact and compact myelin sheaths were observed in the sham group (A2) and 2 W/kg group, while layered myelin sheaths (white arrows) were found in the 4 and 10 W/kg groups (**C2**, **D2**). The figures **A1**, **B1**, **C1**, and **D1** were amplified to 20,000× to better describe the black frame of figures **A**–**D**, respectively. ACx = auditory cortex; RF-EMR = radiofrequency electromagnetic radiation.

1521186x, 2022, 2, Downloaded from https://onlinelibrary.wiley.com/doi/10.1002/bem.22388 by University Of British Columbia, Wiley Online Library on [10/10/2026]. See the Terms and Conditions (https://onlinelibrary.wiley.com/terms-and-conditions) on Wiley Online Library for rules of use; OA articles are governed by the applicable Creative Commons License

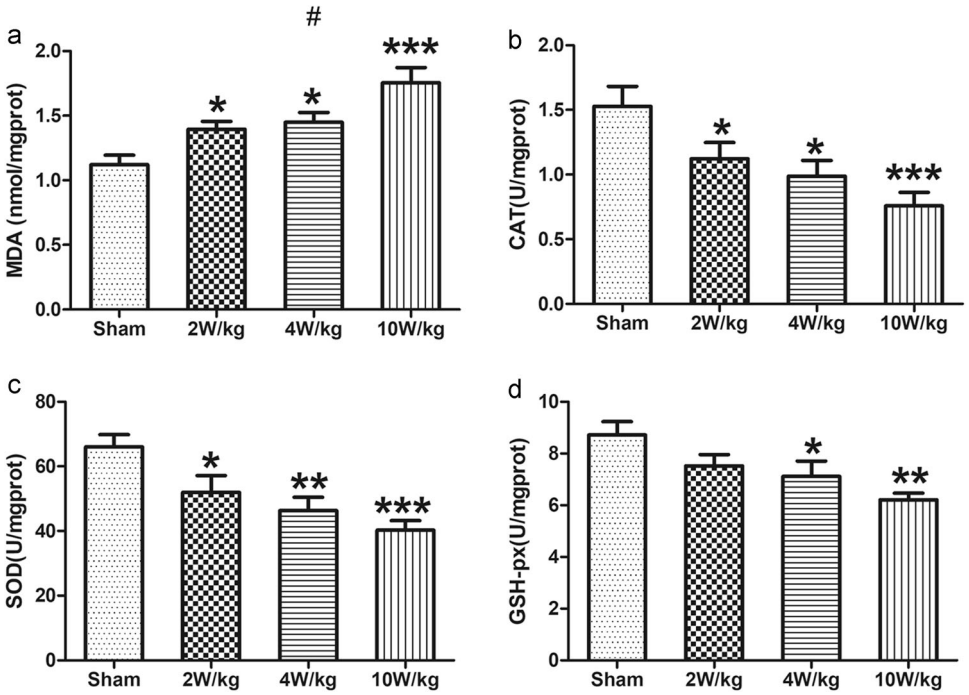


Fig. 4. The effect of 3500 MHz RF-EMR on (**a**) MDA levels, (**b**) CAT activity, (**c**) SOD activity, and (**d**) GSH-px activity in the ACx. The values are expressed as the mean ± SD; $^{*}P < 0.05$, $^{**}P < 0.01$, $^{***}P < 0.001$ versus the sham group. $^{\#}P < 0.05$ versus the 2 W/kg group. ACx = auditory cortex; CAT = catalase; GSH-px = glutathione peroxidase; MDA = malondialdehyde; RF-EMR = radiofrequency electromagnetic radiation; SOD = superoxide dismutase.

1.24- ($P < 0.05$), 1.29- ($P < 0.05$), and 1.56-fold ($P < 0.001$), respectively; CAT activity was decreased by 1.36- ($P < 0.05$), 1.55- ($P < 0.05$), and 2.02-fold ($P < 0.001$), respectively; SOD activity was decreased by 1.27- ($P < 0.05$), 1.43- ($P < 0.01$), and 1.64-fold ($P < 0.001$), respectively; and GSH-px activity was decreased by 1.16-, 1.23- ($p < 0.05$), and 1.41-fold ($P < 0.01$), respectively. The data indicate that as the SAR increased, the activities of SOD, CAT, and GSH-px decreased, and the level of MDA increased.

Cyt *c* Release and Cleaved Caspase-3, Caspase-9 Expression

To determine whether RF-EMR can induce apoptosis, Cyt *c* release, cleaved caspase-3, and caspase-9 expression were detected by IF. Previous studies have shown that Cyt *c* is expressed in neuronal mitochondria and that transport of Cyt *c* from mitochondria to the cytosol indicates apoptosis. As shown in Figure 5, Cyt *c*, which showed slight staining in the sham group, was released from mitochondria into the cytosol in the exposure groups. The fluorescence signal gradually increased as the SAR increased and was the strongest in the 10 W/kg group. As shown in Figures 6 and 7, the caspase-9 and cleaved caspase-3 expression in the exposure groups was higher than that in the sham group, and the expression gradually increased as the SAR increased. The above results indicate that RF-EMR exposure may trigger apoptosis.

DISCUSSION

Previous studies have shown the effect of exposure to RF-EMR of different frequencies and intensities on the eyes, hippocampus, cochlea, and reproductive system. Our study focused for the first time on the effect of acute exposure to high-frequency and high-SAR RF-EMR on the ACx and anxiety-like behavior. The results demonstrated that there were no significant changes in hearing threshold or anxiety. However, we found that acute exposure to 3500 MHz RF-EMR changed the ultrastructures of the ACx, caused Cyt-*c* release from mitochondria, increased the expression of caspase-9 and cleaved caspase-3, and induced oxidative stress.

Activation of the ROS system is relevant to oxidative damage to cellular macromolecules such as lipids, proteins, and nucleic acids, which play a

1521186x, 2022, 2, Downloaded from https://onlinelibrary.wiley.com/doi/10.1002/bem.22388 by University Of British Columbia, Wiley Online Library on [10/10/2026]. See the Terms and Conditions (https://onlinelibrary.wiley.com/terms-and-conditions) on Wiley Online Library for rules of use; OA articles are governed by the applicable Creative Commons License

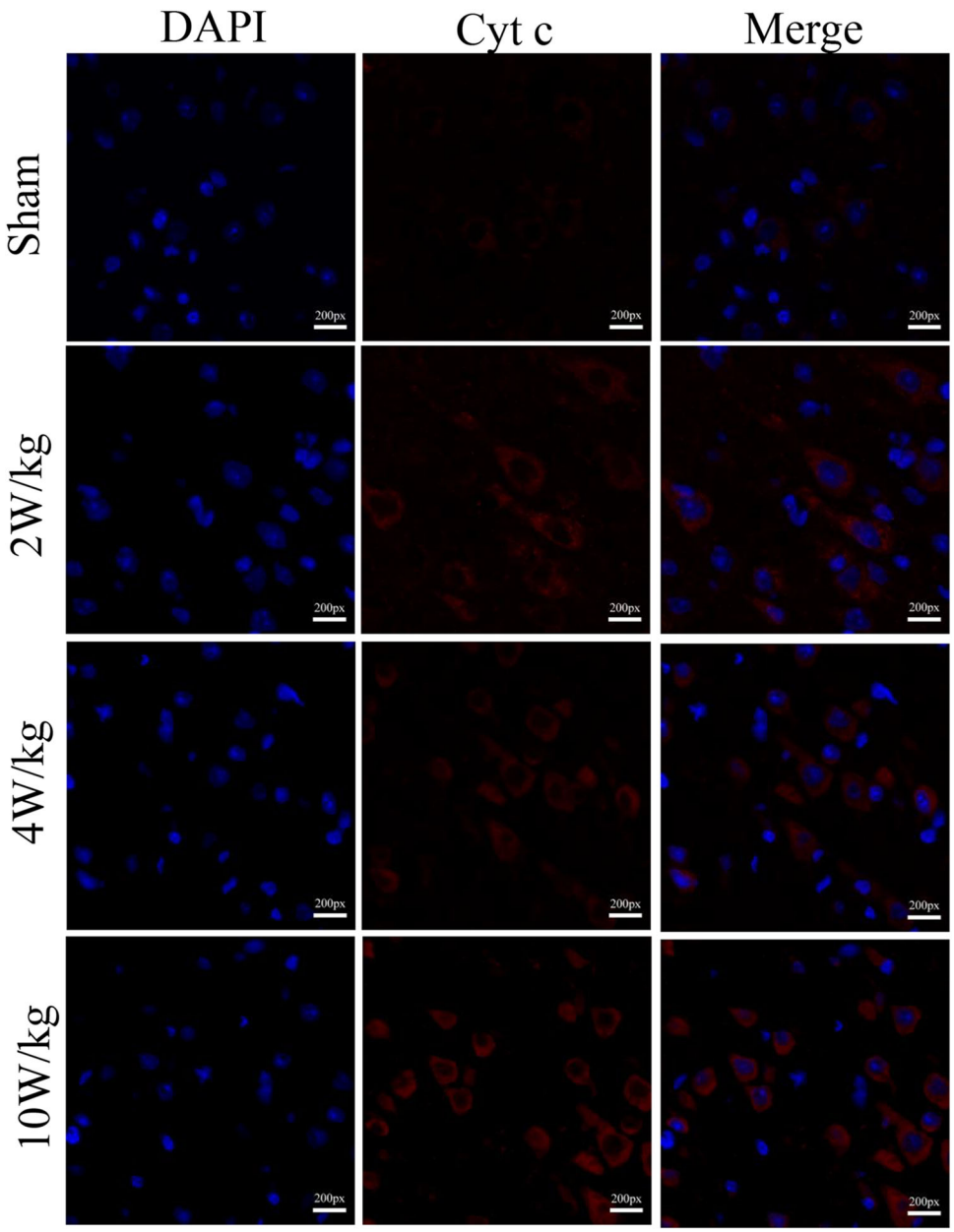


Fig. 5. Cyt *c* release detected by IF (magnification, ×400). The red fluorescence represents Cyt *c* staining, the blue fluorescence represents DAPI staining, and the merged images show Cyt *c* and DAPI double staining in the ACx. ACx = auditory cortex; DAPI = 4′,6-diamidino-2-phenylindole; IF = immunofluorescence.

significant role in the biological effects of RF-EMR. MDA is the breakdown product of the major chain reactions leading to the oxidation of polyunsaturated fatty acids, thus causing oxidative stress [Draper and Hadley, 1990]. However, antioxidant defense systems, including SOD, CAT, and GSH-px, can scavenge this harmful molecule. In the present study, acute exposure to 3500 MHz RF-EMR at an SAR of 2, 4, or 10 W/kg resulted in intensity-dependent increases in free radical load, which subsequently induced oxidative stress in the ACx and weakened the antioxidant defense system. These changes are consistent with previous observations in various cells and tissues [Esmekaya et al., 2011; Salah et al., 2013; Özsobacı et al., 2019]. Additionally, oxidative stress induced by 3500 MHz RF-EMR led to ultrastructural changes in the ACx. Swollen mitochondria were observed in ACx neurons by TEM. In addition, intact and compact

1521186x, 2022, 2, Downloaded from https://onlinelibrary.wiley.com/doi/10.1002/bem.22388 by University Of British Columbia, Wiley Online Library on [10/10/2026]. See the Terms and Conditions (https://onlinelibrary.wiley.com/terms-and-conditions) on Wiley Online Library for rules of use; OA articles are governed by the applicable Creative Commons License

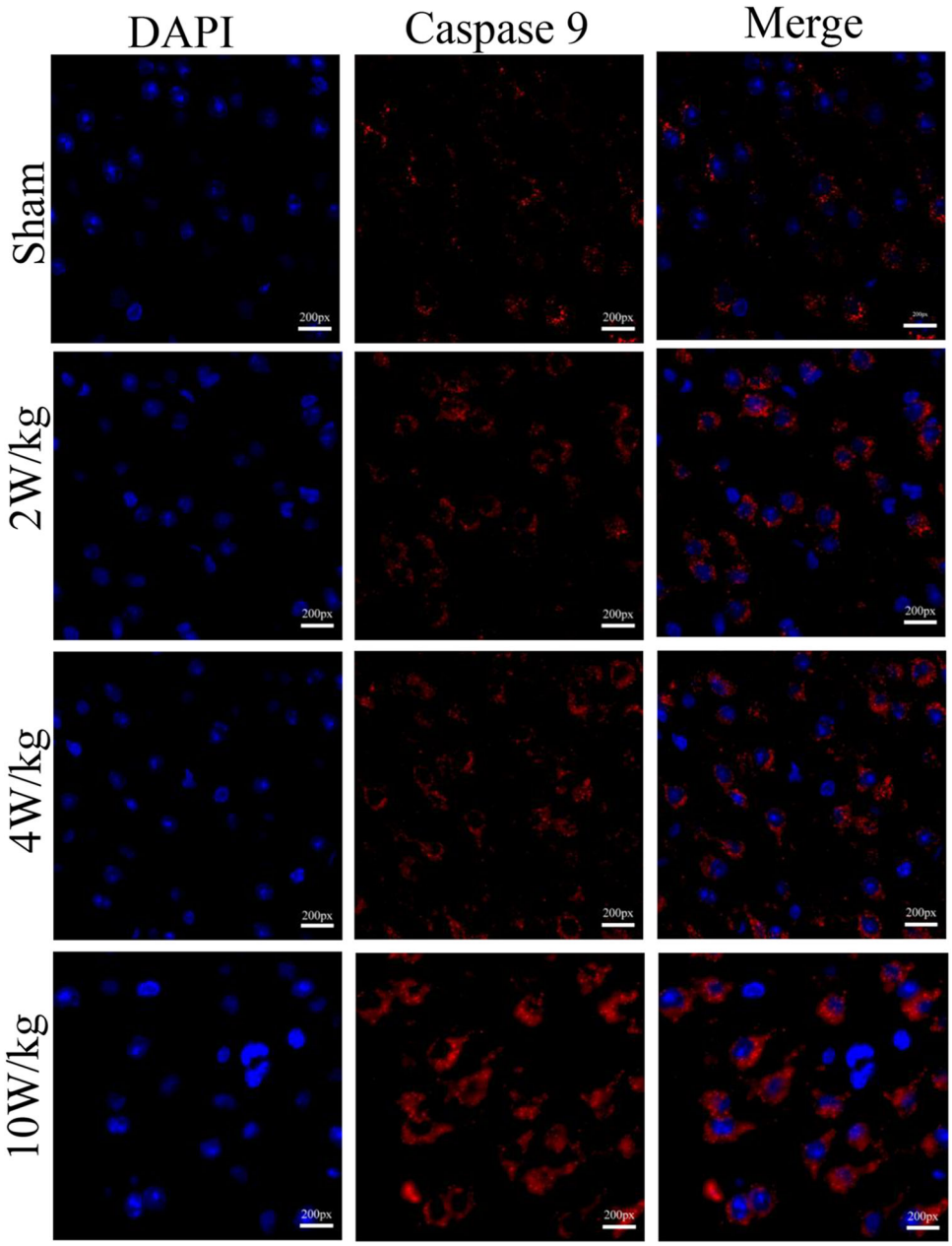


Fig. 6. Caspase 9 expression detected by IF (magnification, ×400). The red fluorescence represents caspase 9 staining, the blue fluorescence represents DAPI staining, and the merged images show caspase 9 and DAPI double staining in the ACx. ACx = auditory cortex; DAPI = 4′,6-diamidino-2-phenylindole; IF = immunofluorescence.

myelin sheaths were observed in the sham and 2 W/kg groups, while layered myelin sheaths were observed in the 4 and 10 W/kg groups. Myelin serves as an electrical insulator for the transmission of electrical signals in the central and peripheral nervous systems and plays critical roles in the development and function of the nervous system [Redmayne and Johansson, 2014; Kim et al., 2017]. This result indicates that RF-EMF exposure at an SAR of 4 or 10 W/kg may damage myelin in the ACx, while RF-EMR at an SAR of 2 W/kg cannot induce damage to myelin. More research is needed to confirm the effect of RF-EMR at different SARs on the nervous system.

Apoptosis is an organized and energy-dependent process in which mitochondria play a crucial regulatory role [Samaiya et al., 2016]. Changes in cellular redox can be part of signal transduction during apoptosis. It has been reported that 1800 MHz

1521186x, 2022, 2, Downloaded from https://onlinelibrary.wiley.com/doi/10.1002/bem.22388 by University Of British Columbia, Wiley Online Library on [10/10/2026]. See the Terms and Conditions (https://onlinelibrary.wiley.com/terms-and-conditions) on Wiley Online Library for rules of use; OA articles are governed by the applicable Creative Commons License

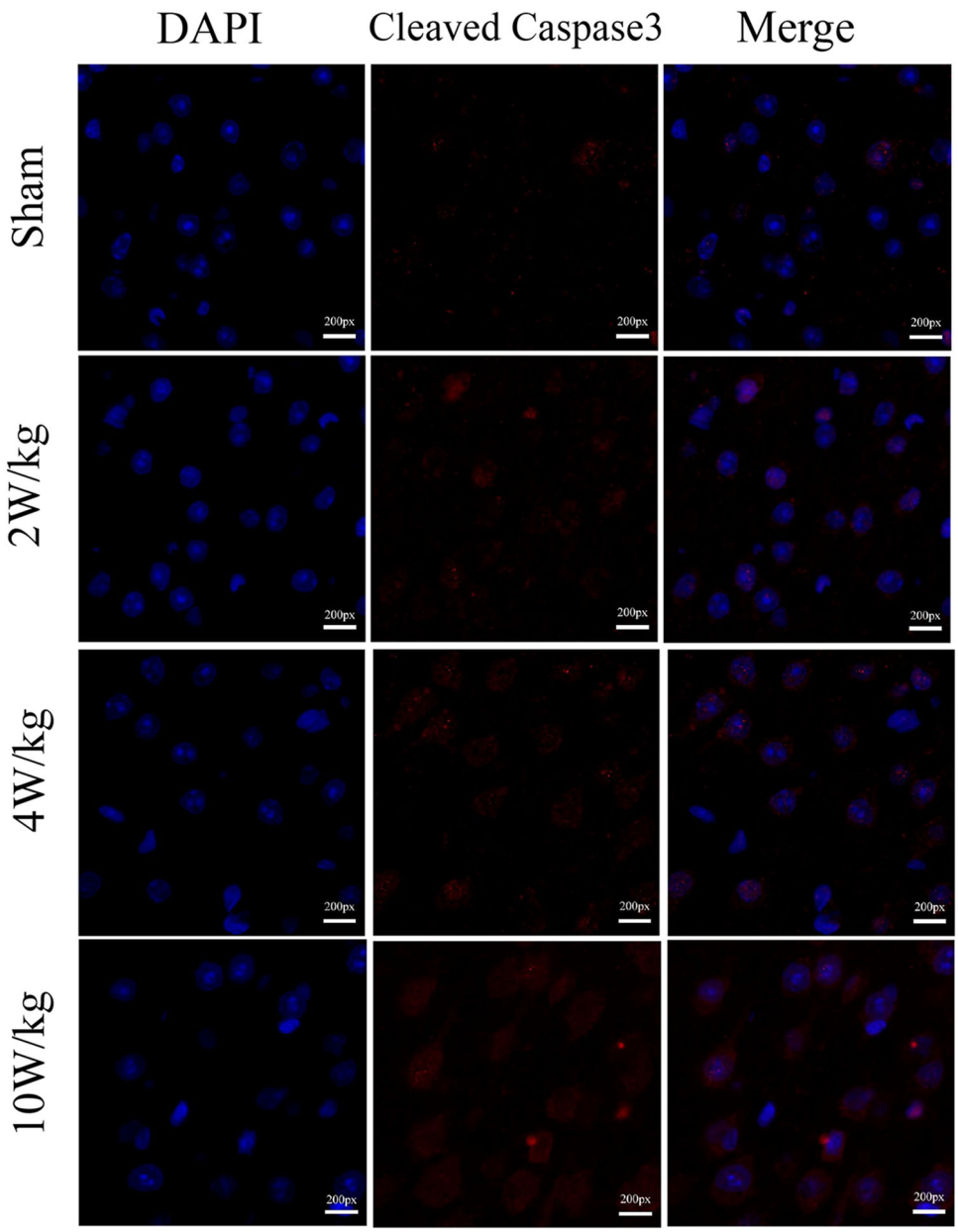


Fig. 7. Cleaved caspase-3 expression detected by IF (magnification, ×400). The red fluorescence represents cleaved caspase-3 staining, the blue fluorescence represents DAPI staining, and the merged images show cleaved caspase-3 and DAPI double staining in the ACx. ACx = auditory cortex; DAPI = 4′,6-diamidino-2-phenylindole; IF = immunofluorescence.

RF-EMR can induce oxidation of the mitochondrial pores, disrupt the mitochondrial membrane potential ($\Delta\psi_m$), and cause Cyt *c* release through overproduction of ROS [Santini et al., 2018]. In the present study, Cyt *c* release from mitochondria into the cytosol, which indicates the opening of the mitochondrial transition pore due to the loss of mitochondrial integrity, was observed in the exposure groups. Cytosolic Cyt *c* acts in concert with apoptosis activating factor-1 (Apaf-1) to activate procaspase-9. Active caspase-9 is an initiator caspase, which in turn activates effector caspases, such as caspase-3 and caspase-7. Caspase-3 is a member of caspase family and plays a central role in the execution phase of cell apoptosis and cleaves the majority of cellular substrates in apoptotic cells. Therefore, we analyzed the expressions of cleaved caspase-3 and caspase-9 by IF. Our results indicate that the caspase-9 and cleaved

1521186x, 2022, 2, Downloaded from https://onlinelibrary.wiley.com/doi/10.1002/bem.22388 by University Of British Columbia, Wiley Online Library on [10/10/2026]. See the Terms and Conditions (https://onlinelibrary.wiley.com/terms-and-conditions) on Wiley Online Library for rules of use; OA articles are governed by the applicable Creative Commons License

caspase-3 expression in the exposure groups was higher than that in the sham group, indicating that exposure to EMR-35000 caused mitochondrial dysfunctions leading to leakage of Cyt-*c* from the mitochondria and activation of intrinsic pathway of apoptosis. Moreover, the significant increase in Cyt *c*, cleaved caspase-3 and caspase-9 expression in the ACx in all exposure groups suggests that the degree of apoptosis induction increased in an SAR intensity-dependent manner.

Many studies have highlighted the contribution of brain mitochondria to psychiatric disorders, including anxiety. Several mitochondrial functions, such as oxidative stress and apoptosis, are altered in individuals with high anxiety levels [Filiou and Sandi, 2019]. In addition, Redmayne and Johansson [2014] reported that myelin damage may induce a variety of symptoms, including irritability, depression, and anxiety. We, therefore, used the OFT to explore whether acute exposure to RF-EMR affects anxiety-like behavior. In our experiment, parameters such as the distance traveled (m), time spent in the inner zone (s), and the average velocity (cm/s) were not significantly changed after exposure to RF-EMR, which indicates that acute exposure to RF-EMR, even at an SAR of 10 W/kg, did not increase the anxiety-like behavior of the guinea pigs in our system. Our results are consistent with previous studies [Kumlin et al., 2007; Júnior et al., 2014], although some studies have reported opposite conclusions [Saikhedkar et al., 2014; Zhang et al., 2017]. The discrepancy may be attributed to the following factors. First, in addition to oxidative stress and apoptosis, changes in energy metabolism, neurosteroid production, and Ca+ concentration in mitochondria are related to anxiety-like behavior. Second, it is well known that neural correlates of anxiety are highly complicated and are related to several brain regions, such as the amygdala, hippocampus, hypothalamus, and cortex. Moreover, different species, apparatuses, and exposure parameters have been used to detect anxiety-like behavior in various studies. Other behavioral tests for anxiety such as elevated plus maze, light-dark transition should be included in future studies.

In addition, although RF-EMR caused changes in the ACx, such as oxidative stress, ultrastructural damage, and cell apoptosis, the ABR thresholds were not increased after acute exposure to 3500 MHz, even at an SAR of 10 W/kg. This indicates that these changes were not sufficient to increase the hearing thresholds measured by the ABR test. Since the ABR test measures retrocochlear function, further studies are needed to investigate whether retrocochlear conduction of nerve impulses is damaged by RF-EMR exposure.

The present study employed an acute exposure model with an exposure period of 72 h. Some people face such exposure under certain circumstances, such as occupational exposure and special emergencies. In our experiment, the activity of the guinea pigs was not limited to reduce the emotional changes that may have been caused by stress interference.

CONCLUSIONS

In summary, oxidative stress is an important mechanism underlying the biological effects of RF-EMR, which can induce ultrastructural damage to the ACx and cell apoptosis through a mitochondria-dependent pathway. The degree of oxidative stress, apoptosis induction, and ultrastructural damage increases in an SAR-dependent manner.

Although RF-EMR does not increase hearing thresholds or induce anxiety in our study, it may alter the hearing thresholds or anxiety level. Also, once the power of RF-EMR-induced oxidative stress reaches considerably above the threshold of auditory perception, it may cause tissue injury. These results provide clues for future research on how to protect the auditory cortex against damage induced by RF-EMR.

ACKNOWLEDGMENTS

The Foundation and Frontier Research Project, Science and Technology Commission, Yuzhong District, Chongqing, China; grant number: 20180105; The Science and Technology Research Program of Chongqing Municipal Education Commission; grant number: KJQN201900433; The National Nature Science Foundation of China; grant number: 81700916.

AUTHOR CONTRIBUTIONS

Honghong Yang carried out the experiments and prepared the manuscript. Shixun Zhong and Wenqi Zuo designed the experiments. All of the authors participated in the data analysis, discussion, and editing and approved the final manuscript.

REFERENCES

Agarwal A, Desai NR, Makker K, Varghese A, Mouradi R, Sabanegh E, Sharma R. 2009. Effects of radiofrequency electromagnetic waves (RF-EMW) from cellular phones on

1521186x, 2022, 2, Downloaded from https://onlinelibrary.wiley.com/doi/10.1002/bem.22388 by University Of British Columbia, Wiley Online Library on [10/10/2026]. See the Terms and Conditions (https://onlinelibrary.wiley.com/terms-and-conditions) on Wiley Online Library for rules of use; OA articles are governed by the applicable Creative Commons License

human ejaculated semen: An in vitro pilot study. Fertil Steril 92:1318–1325.

Akdag M, Dasdag S, Canturk F, Akdag MZ. 2018. Exposure to non-ionizing electromagnetic fields emitted from mobile phones induced DNA damage in human ear canal hair follicle cells. Electromagn Biol Med 37(2):66–75.

Angela PM, Melina PL, Dimitris PC, Dimitris PC. 2003. Radiowave exposure of the human head: Analytical study based on a versatile eccentric spheres model including a brain core and a pair of eyeballs. IEEE Trans Biomed Eng 50:667–676.

Calvente I, Pérez-Lobato R, Núñez MI, Ramos R, Guxens M, Villalba J, Olea N, Fernández MF. 2016. Does exposure to environmental radiofrequency electromagnetic fields cause cognitive and behavioral effects in 10-year-old boys? Bioelectromagnetics 37:25–36.

Carpenter D, Sage C. 2007. BioInitiative Report: A rationale for a biologically-based public exposure standard for electromagnetic fields (ELF and RF). Pathophysiology 16:2009.

Challis L. 2005. Mechanisms for interaction between RF fields and biological tissue. Bioelectromagnetics 26:S98–S106.

Chen CH, Ma QL, Liu C, Deng P, Zhu G, Zhang L, He MD, Lu YH, Duan WX, Pei LP. 2014. Exposure to 1800 MHz radiofrequency radiation impairs neurite outgrowth of embryonic neural stem cells. Sic Rep 4:5103.

Dasdag S, Akdag MZ, Erdal ME, Erdal N, Ay OL, Ay ME, Yilmaz SG, Tasdelen B, Yegin. 2015. Effects of 2.4 GHz radiofrequency radiation emitted from Wi-Fi equipment on microRNA expression in brain tissue. Int J Radiat Biol 91(7):555–561.

Dimitris JP, Olle J, George LC. 2013. Evaluation of specific absorption rate as a dosimetric quantity for electromagnetic fields bioeffects. PLoS One 8:e62663.

Draper H, Hadley M. 1990. Malondialdehyde determination as index of lipid peroxidation. Methods Enzymol 186:421–431.

Dundar B, Cesur G, Comlekci S, Songur A, Gokcimen A, Sahin O, Ulukut O, Yilmaz HR, Sutcu R, Caliskan S. 2009. The effect of the prenatal and post-natal long-term exposure to 50 Hz electric field on growth, pubertal development and IGF-1 levels in female Wistar rats. Toxicol Ind Health 25:479–487.

Esmekaya MA, Ozer C, Seyhan N. 2011. 900 MHz pulse-modulated radiofrequency radiation induces oxidative stress on heart, lung, testis and liver tissues. Gen Physiol Biophys 30:84–89.

Filiou MD, Sandi C. 2019. Anxiety and brain mitochondria: A bidirectional crosstalk. Trends Neurosci 49:573–588.

Fiset C, Rioux FM, Surette ME, Fiset S. 2015. Prenatal iron deficiency in guinea pigs increases locomotor activity but does not influence learning and memory. PLoS ONE 10:e0133168.

Gupta SK, Mesharam MK, Krishnamurthy S. 2018. Electromagnetic radiation 2450 MHz exposure causes cognition deficit with mitochondrial dysfunction and activation of intrinsic pathway of apoptosis in rats. J Biosci 43:263–276.

Hardell L, Sage C. 2008. Biological effects from electromagnetic field exposure and public exposure standards. Biomed Pharmacother 62:104–109.

Júnior LCdC, Guimarães EdSG, Musso CM, Stabler CT, Garcia RMG, Mourão-Júnior CA, Andreazzi AE. 2014. Behavior and memory evaluation of Wistar rats exposed to 1.8 GHz radiofrequency electromagnetic radiation. Neurol Res 36:800–803.

Kim JH, Yu D-H, Huh YH, Lee EH, Kim H-G, Kim HR. 2017. Long-term exposure to 835 MHz RF-EMF induces hyperactivity, autophagy and demyelination in the cortical neurons of mice. Sci Rep 7:41129.

King AJ, Teki S, Willmore BD. 2018. Recent advances in understanding the auditory cortex. F1000Research 7:1555.

Kumlin T, Iivonen H, Miettinen P, Juvonen A, van Groen T, Puranen L, Pitkäaho R, Juutilainen J, Tanila H. 2007. Mobile phone radiation and the developing brain: Behavioral and morphological effects in juvenile rats. Radiat Res 168:471–479.

Leszczynski D, Joenväärä S, Reivinen J, Kuokka R. 2002. Non-thermal activation of the hsp27/p38MAPK stress pathway by mobile phone radiation in human endothelial cells: Molecular mechanism for cancer-and blood-brain barrier-related effects. Differentiation 70:120–129.

Oktay MF, Dasdag S. 2006. Effects of intensive and moderate cellular phone use on hearing function. Electromagn Biol Med 25:13–21.

Oktay MF, Dasdag S, Akdere M, Cureoglu S, Cebe M, Yazicioglu M, Topcu I, Meric F. 2004. Occupational safety: Effects of workplace radiofrequencies on hearing function. Arch Medical Res 35:517–521.

Özgür A, Tümkaya L, Terzi S, Kalkan Y, Erdivanlı ÖÇ, Dursun E. 2015. Effects of chronic exposure to electromagnetic waves on the auditory system. Acta Otolaryngol 135:765–770.

Özsobacı NP, Ergün DD, Tunçdemir M, Özçelik D. 2019. Protective effects of zinc on 2.45 GHz Electromagnetic radiation-induced oxidative stress and apoptosis in HEK293 Cells. Biol Trace Elem Res, 135 1–11.

Ozturan O, Erdem T, Miman MC, Kalcioglu MT, Oncel Sh. 2002. Effects of the electromagnetic field of mobile telephones on hearing. Acta Otolaryngol 122:289–293.

Qin L, Zhang B, Wang Q, Li D, Luo X, Zhong S. 2017. Effect of aldosterone on cochlear Af9 expression and hearing in guinea pig. Acta Otolaryngol 137:903–909.

Redmayne M, Johansson O. 2014. Could myelin damage from radiofrequency electromagnetic field exposure help explain the functional impairment electrohypersensitivity? A review of the evidence. J Toxicol Environ Health B Crit Rev 17:247–258.

Saikhedkar N, Bhatnagar M, Jain A, Sukhwal P, Sharma C, Jaiswal N. 2014. Effects of mobile phone radiation (900 MHz radiofrequency) on structure and functions of rat brain. Neurol Res 36:1072–1079.

Salah MB, Abdelmelek H, Abderraba M. 2013. Effects of olive leave extract on metabolic disorders and oxidative stress induced by 2.45 GHz WIFI signals. Environ Toxicol Pharmacol 36:826–834.

Samaiya PK, Narayan G, Kumar A, Krishnamurthy S. 2016. Neonatal anoxia leads to time dependent progression of mitochondrial linked apoptosis in rat cortex and associated long term sensorimotor deficits. Int J Dev Neurosci 52:55–65.

Santini SJ, Cordone V, Falone S, Mijit M, Tatone C, Amicarelli F, Di, Emidio G. 2018. Role of mitochondria in the oxidative stress induced by electromagnetic fields: Focus on reproductive systems. Oxid Med Cell longev 5076271, 55-65.

Seckin E, Basar FS, Atmaca S, Kaymaz F, Suzer A, Akar A, Sunan E, Koyuncu M. 2014. The effect of radiofrequency radiation generated by a Global System for Mobile Communications source on cochlear development in a rat model. J Laryngol Otol 128:400–405.

1521186x, 2022, 2, Downloaded from https://onlinelibrary.wiley.com/doi/10.1002/bem.22388 by University Of British Columbia, Wiley Online Library on [10/10/2026]. See the Terms and Conditions (https://onlinelibrary.wiley.com/terms-and-conditions) on Wiley Online Library for rules of use; OA articles are governed by the applicable Creative Commons License

Sievert U, Eggert S, Goltz S, Pau H. 2007. Effects of electromagnetic fields emitted by cellular phone on auditory and vestibular labyrinth. Laryngorhinootologie 86:264–270.

Tanaka D, Nakada K, Takao K, Ogasawara E, Kasahara A, Sato A, Yonekawa H, Miyakawa T, Hayashi J-I. 2008. Normal mitochondrial respiratory function is essential for spatial remote memory in mice. Mol Brain 1:21-70.

Thomée S, Härenstam A, Hagberg M. 2011. Mobile phone use and stress, sleep disturbances, and symptoms of depression among young adults—A prospective cohort study. BMC Public Health 11:66.

Tobach E, Gold P. 1966. Behavior of the guinea pig in the open-field situation. Psychol Rep 18:415–425.

Uloziene I, Uloza V, Gradauskiene E, Saferis V. 2005. Assessment of potential effects of the electromagnetic fields of mobile phones on hearing. BMC Public Health 5:39.

Valberg PA, Van Deventer TE, Repacholi MH. 2006. Workgroup report: Base stations and wireless networks—radiofrequency (RF) exposures and health consequences. Environ Health Perspect 115:416–424.

Vecchia P. 2007. Exposure of humans to electromagnetic fields. Standards and regulations. Ann Ist Super Sanita 43:260–267.

Wang K, Lu J, Xing Z, Zhao Q, Hu L, Xue L, Zhang J, Mei Y. 2017. Effect of 1.8 GHz radiofrequency electromagnetic radiation on novel object associative recognition memory in mice. Sci Rep 7:44521.

Wdowiak A, Wdowiak L, Wiktor H. 2007. Evaluation of the effect of using mobile phones on male fertility. Ann Agric Environ Med 14:169–172.

Yorgancilar E, Dasdag S, Akdag MZ, Gun R, Meric F. 2012. Long term effect of 900 MHz radiofrequency radiation exposure on cochlear functions. Biotechnol Biotec EQ 26(6):3397–3401.

Zhang J, Zhang K, Guo L, Chen Q, Gao P, Wang T, Li J, Guo G, Ding G. 2017. Effects of 1.8 GHz Radiofrequency fields on the emotional behavior and spatial memory of adolescent mice. Int J Environ Res Public Health 14:1344.

Zipser B, Schleking A, Kaiser S, Sachser N. 2014. Effects of domestication on biobehavioural profiles: A comparison of domestic guinea pigs and wild cavies from early to late adolescence. Front Zool 11:30.

Zuo W, Hu Y, Yang Y, Zhao X, Zhang Y, Kong W, Kong W. 2015. Sensitivity of spiral ganglion neurons to damage caused by mobile phone electromagnetic radiation will increase in lipopolysaccharide-induced inflammation in vitro model. J Neuroinflammation 12:105.

1521186x, 2022, 2, Downloaded from https://onlinelibrary.wiley.com/doi/10.1002/bem.22388 by University Of British Columbia, Wiley Online Library on [10/10/2026]. See the Terms and Conditions (https://onlinelibrary.wiley.com/terms-and-conditions) on Wiley Online Library for rules of use; OA articles are governed by the applicable Creative Commons License